The ERF11 Transcription Factor Promotes Internode Elongation by Activating Gibberellin Biosynthesis and Signaling[1][OPEN]

Xin Zhou[2], Zhong-Lin Zhang, Jeongmoo Park, Ludmila Tyler[3], Jikumaru Yusuke, Kai Qiu, Edward A. Nam[4], Shelley Lumba, Darrell Desveaux, Peter McCourt, Yuji Kamiya[5], and Tai-ping Sun*

Department of Biology, Duke University, Durham, North Carolina 27705 (X.Z., Z.-L.Z., L.T., J.P., E.A.N., T.-p.S.); RIKEN Plant Science Center, Yokohama, Kanagawa 230-0045, Japan (J.Y., Y.K.); Department of Cell and Systems Biology, University of Toronto, Ontario M5S 3B2, Canada (S.L., D.D., P.M.); Centre for the Analysis of Genome Evolution and Function, University of Toronto, Ontario M5S 3B2, Canada (D.D.); and State Key Laboratory of Genetic Engineering and Fudan Institute of Plant Biology, School of Life Sciences, Fudan University, Shanghai 200433, China (K.Q.)

ORCID IDs: 0000-0003-2555-5929 (J.P.); 0000-0002-7950-7001 (E.A.N.); 0000-0003-4415-520 (Y.K.).

The phytohormone gibberellin (GA) plays a key role in promoting stem elongation in plants. Previous studies show that GA activates its signaling pathway by inducing rapid degradation of DELLA proteins, GA signaling repressors. Using an activation-tagging screen in a reduced-GA mutant *ga1-6* background, we identified AtERF11 to be a novel positive regulator of both GA biosynthesis and GA signaling for internode elongation. Overexpression of AtERF11 partially rescued the dwarf phenotype of *ga1-6*. AtERF11 is a member of the ERF (ETHYLENE RESPONSE FACTOR) subfamily VIII-B-1a of ERF/AP2 transcription factors in Arabidopsis (*Arabidopsis thaliana*). Overexpression of AtERF11 resulted in elevated bioactive GA levels by up-regulating expression of *GA3ox1* and *GA20ox* genes. Hypocotyl elongation assays further showed that overexpression of AtERF11 conferred elevated GA response, whereas loss-of-function *erf11* and *erf11 erf4* mutants displayed reduced GA response. In addition, yeast two-hybrid, coimmunoprecipitation, and transient expression assays showed that AtERF11 enhances GA signaling by antagonizing the function of DELLA proteins via direct protein-protein interaction. Interestingly, AtERF11 overexpression also caused a reduction in the levels of another phytohormone ethylene in the growing stem, consistent with recent finding showing that AtERF11 represses transcription of ethylene biosynthesis *ACS* genes. The effect of AtERF11 on promoting GA biosynthesis gene expression is likely via its repressive function on ethylene biosynthesis. These results suggest that AtERF11 plays a dual role in promoting internode elongation by inhibiting ethylene biosynthesis and activating GA biosynthesis and signaling pathways.

Bioactive gibberellin (GA), a diterpenoid compound, is an allosteric inducer of its nuclear receptor GIBBERELLIN INSENSITIVE DWARF1 (GID1; Ueguchi-Tanaka et al., 2005; Murase et al., 2008; Shimada et al., 2008). Acting downstream of GID1, the DELLA proteins are transcription regulators that repress GA signaling and restrict plant growth by causing transcriptional reprogramming (Ueguchi-Tanaka et al., 2007). Binding of GA to GID1 enhances the interaction between GID1 and DELLA, resulting in rapid degradation of DELLAs via the ubiquitin-proteasome pathway. In Arabidopsis (*Arabidopsis thaliana*), DELLAs are members of the GRAS (GA INSENSITIVE [GAI], REPRESSOR OF *ga1-3* [RGA], and SCARECROW) family of regulatory proteins (Tian et al., 2004). Like all GRAS family members, DELLA contains a conserved C-terminal GRAS domain that confers the transcription regulator function. The unique DELLA domain in the N terminus of the protein is required for GA-induced degradation via GID1 binding (Dill et al., 2001; Itoh et al., 2002; Griffiths et al., 2006; Murase et al., 2008); this domain is absent in other GRAS family members. Among the five DELLAs (RGA, GAI, RGA-LIKE1 [RGL1], RGL2, and RGL3) in Arabidopsis, RGA and GAI are the major DELLAs for regulating GA-induced vegetative growth (Dill and Sun, 2001; King et al., 2001).

Recent studies also show that DELLAs integrate GA and other signaling pathways by antagonizing or enhancing functions of key regulators in other pathways via direct protein-protein interactions (Xu et al., 2014; Daviere and Achard, 2016). Most of the DELLA-interacting proteins are transcription factors or transcription regulators. Examples of DELLA-inhibited transcription factors/regulators include bHLH transcription factors, PIFs, in light signaling (de Lucas et al., 2008; Feng et al., 2008); the jasmonic acid (JA) signaling repressors, JAZs (Hou et al., 2010; Yang et al., 2012); ETHYLENE INSENSITIVE3 (EIN3), an ethylene signaling activator (An et al., 2012); and BRASSINAZOLE-RESISTANT1, a brassinosteroid signaling activator (Bai et al., 2012). DELLA-activated transcription factors include type-B ARABIDOPSIS RESPONSE REGULATORs (Marín-de la Rosa et al., 2015), ABSCISIC ACID INSENSITIVE3 (ABI3), and ABI5 (Lim et al., 2013). Other types of DELLA interactors include chromatin-remodeling complexes

(Switch/Suc Nonfermenting, and a Chromodomain-Helicase-DNA-binding domain-containing protein PICKLE; Sarnowska et al., 2013; Zhang et al., 2014), RING domain proteins BOTRYTIS SUSCEPTIBLE1 INTERACTOR (BOI) and BOI-RELATED GENEs (BRG1, BRG2, and BRG3; Park et al., 2013), and subunits of the prefoldin complex for tubulin folding (Locascio et al., 2013). These findings indicate that protein-protein interaction is a central regulatory mechanism in DELLA-modulated plant development. Although a number of DELLA-interacting proteins have been reported, our current knowledge on how DELLAs regulate plant growth and development is still limited.

To uncover new regulators of the GA pathway, we performed an activation-tagging mutant screen and identified AtERF11, a member of the ERF (ETHYLENE RESPONSE FACTOR)/AP2 (APETALA2) family (Nakano et al., 2006), as a novel regulator of GA pathway. Our results show that AtERF11 promotes cell elongation by increasing bioactive GA accumulation. ERF11 also enhances GA responses by directly antagonizing DELLA function through protein-protein interaction. Interestingly, ERF11 has been reported to repress genes encoding ethylene biosynthetic enzymes (ACC synthases [ACSs]) (Li et al., 2011). Therefore, ERF11 may provide a molecular link between GA and ethylene pathways in modulating internode elongation.

RESULTS

Identification of ERF11 as a Positive Regulator of Internode Elongation through an Activation-Tagging Approach

To identify positive components of the GA signaling pathway, an activation-tagging mutant screen was employed to isolate mutants that grow taller than parental *ga1-6* plants. The *ga1-6* mutant is a GA-deficient semidwarf because of a missense mutation in *GA1* (*AtCPS*) that encodes *ent*-copalyl diphosphate synthase (CPS) for GA biosynthesis (Sun et al., 1992; Sun and Kamiya, 1994). We reasoned that enhanced expression of positive regulators of the GA pathway would lead to a taller phenotype in this semidwarf mutant background. The *ga1-6* plants (backcrossed four times to Col-0) were transformed with *Agrobacterium tumefaciens* that carried four copies of *35S* transcriptional enhancers linked to a constitutively expressed BASTA resistance gene (Weigel et al., 2000). Approximately 12,500 T1 transformants were screened for increased final height. Among the mutants identified, mutant #279-2 was dramatically taller than the parental *ga1-6* plants, an average height of 28.5 cm versus 18.3 cm (Fig. 1, A and B).

The #279-2 mutant contains a single T-DNA insertion site, as the linked BASTA resistance gene segregated 3:1 in the T2 generation. Thermal asymmetric interlaced PCR (TAIL-PCR) revealed that the activation tag in #279-2 is inserted in chromosome 1 between At1g28360 and At1g28370, which encode two members of the ERF family, AtERF12 and AtERF11, respectively (Supplemental Fig. S1A). RT-qPCR further showed that the transcript levels of *AtERF11* (At1g28370) were 18.3-fold higher in the mutant #279-2 than in the *ga1-6* control (Fig. 1C). In contrast, the expression levels of the other two adjacent genes, At1g28360 (*AtERF12*) and At1g28375 (an expressed endomembrane protein), were unchanged or only 3-fold higher, respectively, in #279-2 compared to *ga1-6* (Supplemental Fig. S1A). To verify whether overexpression of ERF11 causes the mutant phenotype of #279-2, we generated transgenic *ga1-6* plants carrying CaMV *35S* promoter:*HA-ERF11-GFP* (*ERF11-OE* lines). Indeed, the final heights of these *ERF11-OE* lines correlated with ERF11 protein levels in these plants (Fig. 1, A and D). The line with the highest ERF11 protein expression (#1-1) reached a similar final height as #279-2 (Fig. 1A), indicating that overexpression of *ERF11* is responsible for the observed tall phenotype. Mutant #279-2 will be referred to as *erf11-1D ga1-6* in the rest of this report; the homozygous *erf11-1D ga1-6* double mutant in the T5 generation was used for all data presented here.

To understand better the effect of overexpression of *ERF11* on stem elongation, the inflorescence stem of *erf11-1D ga1-6* was characterized in more detail. *erf11-1D ga1-6* produced a similar number of siliques as *ga1-6* (Supplemental Fig. S1B), but with 82.3% longer internodes that contributed to the increased final height of the mutant (Fig. 1, E and F). Scanning electron microscopy analysis revealed that the longer internode in *erf11-1D ga1-6* is caused by increased cell length (Fig. 1, G and H), but not greater cell numbers (Supplemental Fig. S1C). A previous study indicated that *ERF11* is expressed ubiquitously in different tissues of wild-type plants; however, the highest transcript levels were detected in leaves and stems (Yang et al., 2005).

[1] This work was supported by the National Science Foundation (IOS-0641548 and MCB-0923723), the U.S. Department of Agriculture (2014-67013-21548), the National Institutes of Health (R01 GM100051), and the Canada Research Chair-National Sciences and Engineering Research Council (grant no. 00003714).

[2] Present address: Department of Biology, College of Life and Environmental Sciences, Shanghai Normal University, Shanghai 200234, China.

[3] Present address: Department of Biochemistry and Molecular Biology, University of Massachusetts, Amherst, MA 01003.

[4] Present address: Department of Biology, University of St. Thomas, Houston, TX 77006.

[5] Present address: RIKEN Center for Sustainable Resource Science, Wako, Saitama 351-0198, Japan.

* Address correspondence to tps@duke.edu.

The author responsible for distribution of materials integral to the findings presented in this article in accordance with the policy described in the Instructions for Authors (www.plantphysiol.org) is: Tai-ping Sun (tps@duke.edu).

X.Z., Z.Z., J.P., and T.S. designed the research; X.Z., Z.Z., L.T., J.Y., K.Q., J.P., and E.A.N. performed research; X.Z., Z.Z., J.P., J.Y., Y.K., and T.S. analyzed data; S.L., D.D., and P.M. provided experimental materials and shared unpublished results; X.Z., Z.Z., and T.S. wrote the manuscript.

[OPEN] Articles can be viewed without a subscription.

www.plantphysiol.org/cgi/doi/10.1104/pp.16.00154

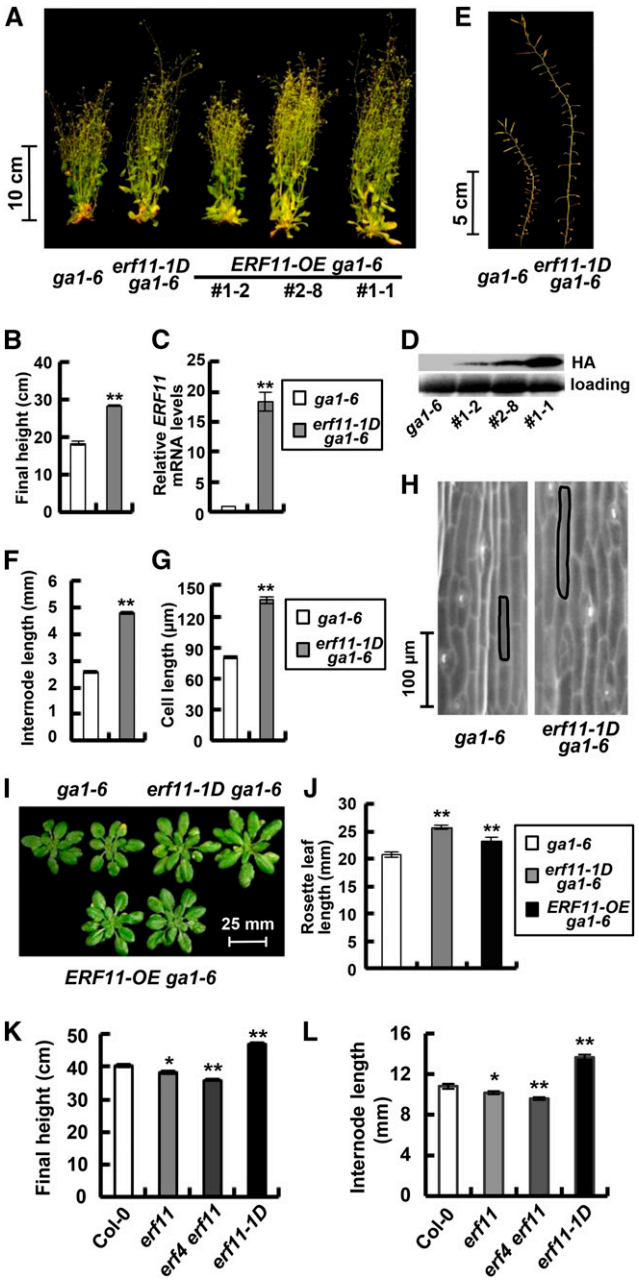

Figure 1. Overexpression of *ERF11* increased plant height by promoting cell elongation. A, The tall phenotype of mutant #279-2 (renamed *erf11-1D ga1-6*) was recapitulated by expressing *35S:HA-ERF11-GFP* (*ERF11-OE*) in the *ga1-6* background. Plant image was taken 50 d after planting. #1-1, #1-2, and #2-8 are three independent *ERF11-OE ga1-6* transgenic lines (T2 generation). B, The final height of *erf11-1D ga1-6* is taller than *ga1-6*. $n = 24$. C, The *ERF11* transcript levels are significantly higher in *erf11-1D ga1-6* than in *ga1-6*. Data represent RT-qPCR results using RNA isolated from 8-d-old seedlings. A GA-nonresponsive gene (At4g33380) was used to normalize different samples. Means ± SE of four repeats (from two biological replicas, two technical repeats each) are shown. The level in *ga1-6* was set to 1. D, HA-ERF11-GFP protein levels correlated with the plant heights in A. The immunoblot contains proteins from 8-d-old seedlings of three transgenic *ERF11-OE ga1-6* lines as described in A and was probed with an anti-HA antibody. The bottom panel shows equal loading by Ponceau staining. E and F, Internodes in *erf11-1D ga1-6* were longer than in *ga1-6*. Average internode lengths of 70-d-old *ga1-6* and *erf11-1D ga1-6* were calculated by dividing the length of the primary stem from the apex to the last secondary inflorescence with the total numbers of nodes. $n = 24$. G and H, The average epidermal cell length in the primary stem of *erf11-1D ga1-6* is longer than in *ga1-6*. In G, $n \geq 600$. H, scanning electron microscopy images of the internodes of 70-d-old plants. A representative cell in each line was outlined. I and J, *erf11-1D ga1-6* and *ERF11-OE ga1-6* double homozygous mutants have larger rosette leaves than *ga1-6*. Images in I show 33-d-old plants. In J, $n = 20$. K and L, The final heights (K) and internode lengths (L) of *erf11* and *erf4 erf11* mutants are shorter than those of the wild type. $n = 24$. In B, C, F, G, and J to L, data are means ± SE. $^*P < 0.05$; $^{**}P < 0.01$.

Consistent with this *ERF11* expression pattern, the rosette leaves of *erf11-1D ga1-6* were 22.7% larger than *ga1-6* (Fig. 1, I and J). In addition to the longer internode length and larger rosette size, *erf11-1D ga1-6* flowered slightly earlier and displayed increased fertility compared to *ga1-6* (Supplemental Table S1).

AtERF11 is a member of the ERF subfamily VIII-B-1a of ERF/AP2 transcription factors. There are eight members in this subfamily (ERF3, 4, and 7–12); each of them contains an ERF/AP2 domain and a transcription repression EAR motif (DLNxxP; McGrath et al., 2005; Nakano et al., 2006). Recently, AtERF11 was shown to inhibit ethylene biosynthesis by binding to the promoters of two ACC synthase genes *ACS2* and *ACS5* to repress their expression (Li et al., 2011). Furthermore, overexpression of another VIII-B-1a ERF member, AtERF4, confers reduced ethylene sensitivity in hypocotyl growth (Yang et al., 2005). Similar to *erf11-1D ga1-6*, overexpression of *AtERF4* or *AtERF8* (another close homolog of *ERF11* in the same subfamily) also resulted in increased final height in the *ga1-6* background (Supplemental Fig. S1D). We also generated the *erf11-1D* single mutant by backcrossing *erf11-1D ga1-6* to the wild-type Col-0 and found that *erf11-1D* is taller with 26.5% longer internodes than the wild-type (Fig. 1, K and L). Moreover, the *erf11* knockout mutant showed slightly shorter final height and internode length compared with wild-type Col-0; the *erf11 erf4* double homozygous mutant displayed even shorter stems compared to Col-0 and the *erf11* single mutant (Fig. 1, K and L). Consistent with the shorter stem phenotype, the rosette leaf length of the *erf11 erf4* double mutant was slightly reduced comparing with the wild type (Supplemental Fig. S1E). These results indicated that ERF11 and its close homologs share redundant function in promoting stem elongation and rosette leaf expansion.

Overexpression of *ERF11* Causes Elevated Bioactive GA_4 and Reduced Ethylene Levels in the Growing Internodes

To determine whether the longer internodes of *erf11-1D ga1-6* are caused by increased levels of bioactive GAs, we first analyzed the transcript levels of GA biosynthesis and catabolism genes that are important for vegetative growth (Mitchum et al., 2006; Rieu et al.,

2008a, 2008b) by RT-qPCR. We found that expression of several GA biosynthesis genes, including *GA20ox1*, *GA20ox2*, and *GA3ox1*, was up-regulated in the internodes of *erf11-1D ga1-6* compared with *ga1-6*, while a GA catabolism gene, *GA2ox6*, was down-regulated in *erf11-1D ga1-6* (Fig. 2A). In contrast, *GA3ox2* mRNA levels were not altered (Fig. 2A). GA analysis further showed that the GA_4 level in the rosette leaves of *erf11-1D ga1-6* was about 2-fold higher than that in *ga1-6* (Fig. 2B). Our previous study showed that a 2-fold reduction in GA_4 levels in the Arabidopsis rosette leaves could lead to a 2-fold reduction in the final plant height (Mitchum et al., 2006).

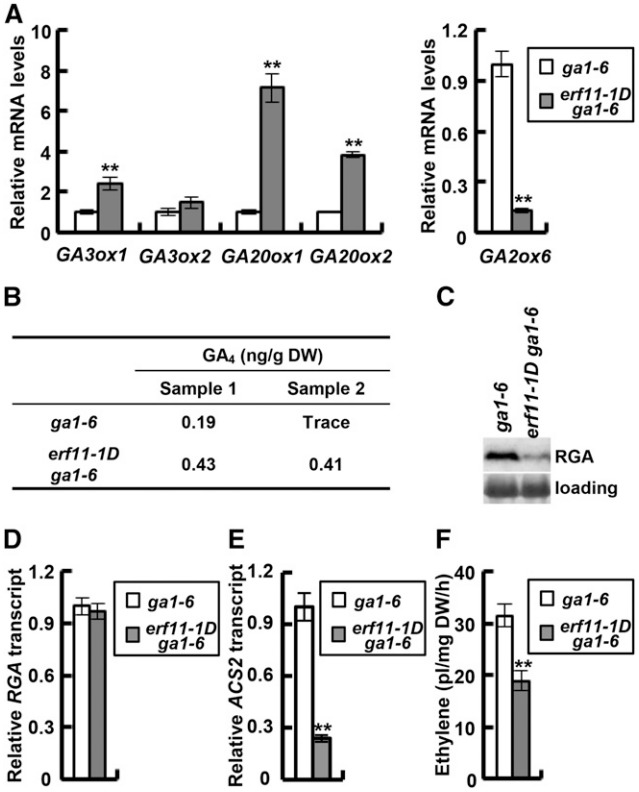

Figure 2. Elevated bioactive GA levels and reduced ethylene levels in *erf11-1D ga1-6*. A, Relative mRNA levels of GA biosynthesis genes (left panel) and GA catabolism gene (right panel) in the internodes of *ga1-6* and *erf11-1D ga1-6*. Data represent means ± SE of four repeats. $^{**}P <$ 0.01. The levels in *ga1-6* were set to 1. B, GA_4 levels (ng/g dry weight) in *erf11-1D ga1-6* were elevated comparing to *ga1-6*. GA_4 contents in rosette leaves of 33-d-old plants were analyzed using two biological repeats. Due to very low levels of bioactive GA_4 content in the *ga1-6* background, we were unable to measure GA_4 accurately in one of the *ga1-6* repeats (test 2), which had trace amounts of GA_4 estimated to be <0.27 ng/g dry weight. C, RGA protein levels were reduced in the internodes of *erf11-1D ga1-6* compared to *ga1-6*. Proteins were extracted from internodes of 50-d-old plants, and immunoblotting was performed with affinity-purified anti-RGA antibodies. The bottom panel shows equal loading by Ponceau staining. D, The *RGA* transcript levels were similar in the internodes of *ga1-6* and *erf11-1D ga1-6*. Data represent means ± SE of four repeats. E, The *ACS2* transcript levels in the internodes of *erf11-1D ga1-6* were reduced in comparison to *ga1-6*. Data represent means ± SE of four repeats. $^{**}P < 0.01$. F, Ethylene production (pL/mg dry weight/h) from the internodes of 50-d-old plants. Data represent means ± SE of four repeats. Similar results were obtained using another set of samples. $^{**}P < 0.01$.

Consistent with the elevated GA levels in *erf11-1D ga1-6*, the amounts of RGA protein (an Arabidopsis DELLA) in the internodes of *erf11-1D ga1-6* were much lower than in *ga1-6* (Fig. 2C), even though *RGA* mRNA levels were not altered by *erf11-1D* (Fig. 2D). Taken together, overexpression of ERF11 in *erf11-1D ga1-6* caused elevated bioactive GA_4 levels through up-regulation of GA biosynthesis genes and down-regulation of a GA catabolism gene, which subsequently led to DELLA degradation and internode growth.

Being an EAR-containing transcription repressor, ERF11 is unlikely to up-regulate expression of GA biosynthesis genes directly. Instead, the elevated GA levels and longer internodes of *erf11-1D ga1-6* may be due to reduced ethylene levels because ERF11 is known to inhibit ethylene biosynthesis by down-regulating *ACS2* and *ACS5* transcription (Li et al., 2011) and enhanced ethylene signaling decreases bioactive GA levels in Arabidopsis rosette plants (Achard et al., 2007). To test this possibility, the transcript levels of *ACS2* in the internodes of *erf11-1D ga1-6* and *ga1-6* were analyzed by RT-qPCR. As predicted, expression of *ACS2* was approximately 5-fold lower in the internodes of *erf11-1D ga1-6* than in *ga1-6* (Fig. 2E). Moreover, the ethylene production in internodes of *erf11-1D ga1-6* was 60% lower than in *ga1-6* (Fig. 2F). Consistently, *erf11-1D* displayed reduced ethylene response (Supplemental Fig. S1F), whereas *erf11* and *erf4 erf11* showed increased ethylene response (Supplemental Fig. S1G). These results indicated that the taller phenotype caused by overexpression of *ERF11* is due to elevated bioactive GA_4 levels and decreased ethylene levels.

ERF11 Positively Regulates GA Responses

The above data indicated that ERF11 promotes bioactive GA accumulation. Interestingly, our hypocotyl elongation assays showed that ERF11 also enhances GA response (Fig. 3; Supplemental Fig. S2A). The *erf11* single mutant displayed slightly reduced GA response compared to the wild type, and the *erf11 erf4* double mutant showed a further reduction in GA response (Fig. 3, A and C). Consistent with these results, overexpression of ERF11 (due to *erf11-1D*) caused an elevated GA response; both the double mutant *erf11-1D ga1-6* and the single *erf11-1D* mutant displayed increased GA response compared to *ga1-6* and Col-0, respectively (Fig. 3, B and D; Supplemental Fig. S2A). We also examined RGA protein levels in seedlings of *ga1-6* and *erf11-1D ga1-6* in response to GA treatments. Supplemental Figure S2B shows that RGA levels decreased in both lines in response to GA treatments, although RGA accumulated to lower levels in *erf11-1D ga1-6* than in *ga1-6* when untreated or with 0.01 μM

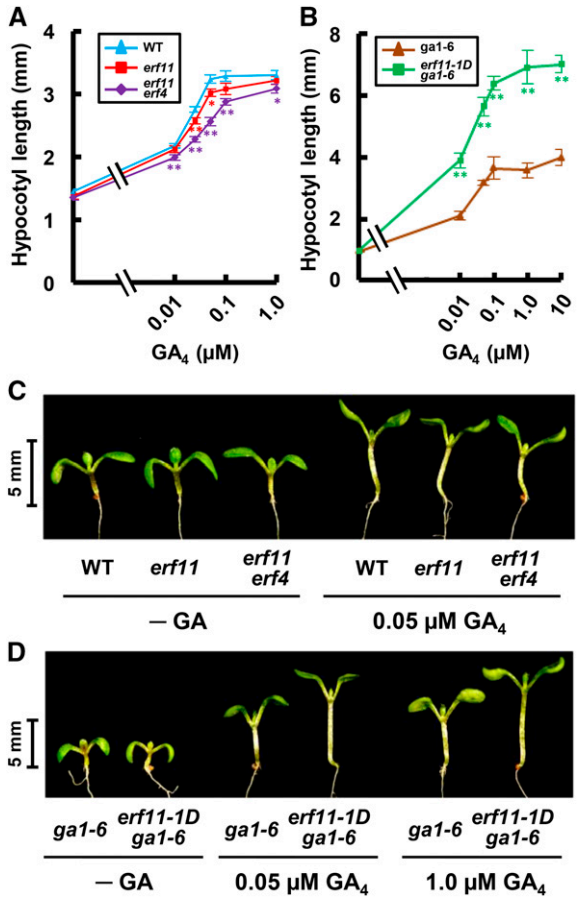

Figure 3. Loss-of-function *erf* mutants displayed reduced GA response, whereas overexpression of *ERF11* increased GA response. A and B, Hypocotyl elongation assays of 4-d-old seedlings grown in different GA concentrations under continuous light (50 μmol m^{-2} s^{-1}). *$P < 0.05$; **$P < 0.01$. C, *erf11* and *erf11 erf4* displayed shorter hypocotyl length in the presence of 0.05 μM GA_4, but not in the untreated control (–GA). Image shows 4-d-old seedlings. D, *erf11-1D ga1-6* showed longer hypocotyl length with 0.05 and 1 μM GA_4 treatment, but not in the untreated control. Image shows 4-d-old seedlings.

GA_4. This is consistent with the elevated GA content in *erf11-1D ga1-6*. These results indicate that ERF11 functions as a positive regulator of both GA production and GA signaling.

ERF11 Antagonizes DELLA Function via Protein-Protein Interaction

To place ERF11 in the GA signaling pathway, genetic interactions between ERF11 and RGA were examined by double mutant analysis. *rga-Δ17* is a transgenic line that expresses a dominant active form of RGA, which lacks a 17-amino acid motif within the DELLA domain that is required for GA-induced degradation (Dill et al., 2001). *rga-Δ17* displays a severe dwarf phenotype, while *erf11-1D* has longer internodes than the wild type. The use of *rga-Δ17* in the double mutant analysis allowed us to uncouple the GA response activity from GA biosynthesis so that we could examine the direct role of ERF11 in the GA response. Because homozygous *rga-Δ17* plants are sterile and grow extremely slowly, we compared phenotypes of the semidwarf hemizygous *rga-Δ17* in the homozygous *erf11-1D* background (referred to as *erf11-1D rga-Δ17*) to the hemizygous *rga-Δ17*. We found that the final height of *erf11-1D rga-Δ17* was 30% taller than *rga-Δ17* (Fig. 4A; Supplemental Fig. S3A), and the internode length of *erf11-1D rga-Δ17* was 46% longer than that of *rga-Δ17* (Supplemental Fig. S3B), whereas the average number of siliques of *erf11-1D rga-Δ17* was similar to that of *erf11-1D* (Supplemental Fig. S3C). These results indicated that *erf11-1D* partially rescued the dwarf phenotype of *rga-Δ17*, suggesting that *erf11-1D* either inhibits rga-Δ17 protein accumulation or activity, or acts downstream of RGA. However, rga-Δ17 protein levels in the internodes of *rga-Δ17* and *erf11-1D rga-Δ17* were similar (Fig. 4B), indicating that the longer internodes in *erf11-1D rga-Δ17* were not caused by reduced rga-Δ17 accumulation.

We then tested whether *erf11-1D* inhibits RGA activity by direct protein-protein interaction, a known regulatory mechanism for DELLA and its interactors (Xu et al., 2014; Daviere and Achard, 2016). Our yeast two-hybrid assays showed that the GRAS domain of RGA directly interacts with ERF11 minus the EAR motif (Fig. 4C). No interaction was detected between RGA and the full-length ERF11, presumably because the transcription repression mediated by the EAR motif interfered with reporter gene expression. We also observed interactions between RGA and three ERF11 close homologs ERF4, ERF8, and ERF10 (in subgroup VIII-B-1a). However, RGA did not interact with ERF88, which belongs to a different subgroup VIII-B-1b (Fig. 4C), suggesting that RGA specifically interacts with ERFs in the VIII-B-1a subfamily. RGA and GAI are the major DELLA proteins that control stem elongation (Dill and Sun, 2001; King et al., 2001). We found that GAI also interacted with ERF11, ERF4, ERF8, and ERF10 in yeast two-hybrid assays (Supplemental Fig. S4).

To confirm ERF11-RGA interaction in planta, we performed coimmunoprecipitation (co-IP) assays by transiently coexpressing *35S:cMyc-ERF11* (or *ERF8*) and *35S:HA-RGA* constructs in leaves of *Nicotiana benthamiana* through *Agrobacterium*-mediated transformation. Tissues infiltrated with *35S:HA-RGA* alone or coinfiltrated with *35S:cMyc-GUS-NLS* served as negative controls. Immunoprecipitation was performed using anti-cMyc antibody-conjugated agarose beads. Figure 4D shows that HA-RGA was coimmunoprecipitated when it was coexpressed with cMyc-ERF11 (–EAR) or cMyc-ERF8 (–EAR), but not when it was expressed alone or coexpressed with cMyc-GUS-NLS. These co-IP assays further support the idea that ERF11 and its close homologs directly interact with RGA. To test whether overexpression of ERF11 inhibits DELLA function, we then examined transcript levels of DELLA target genes

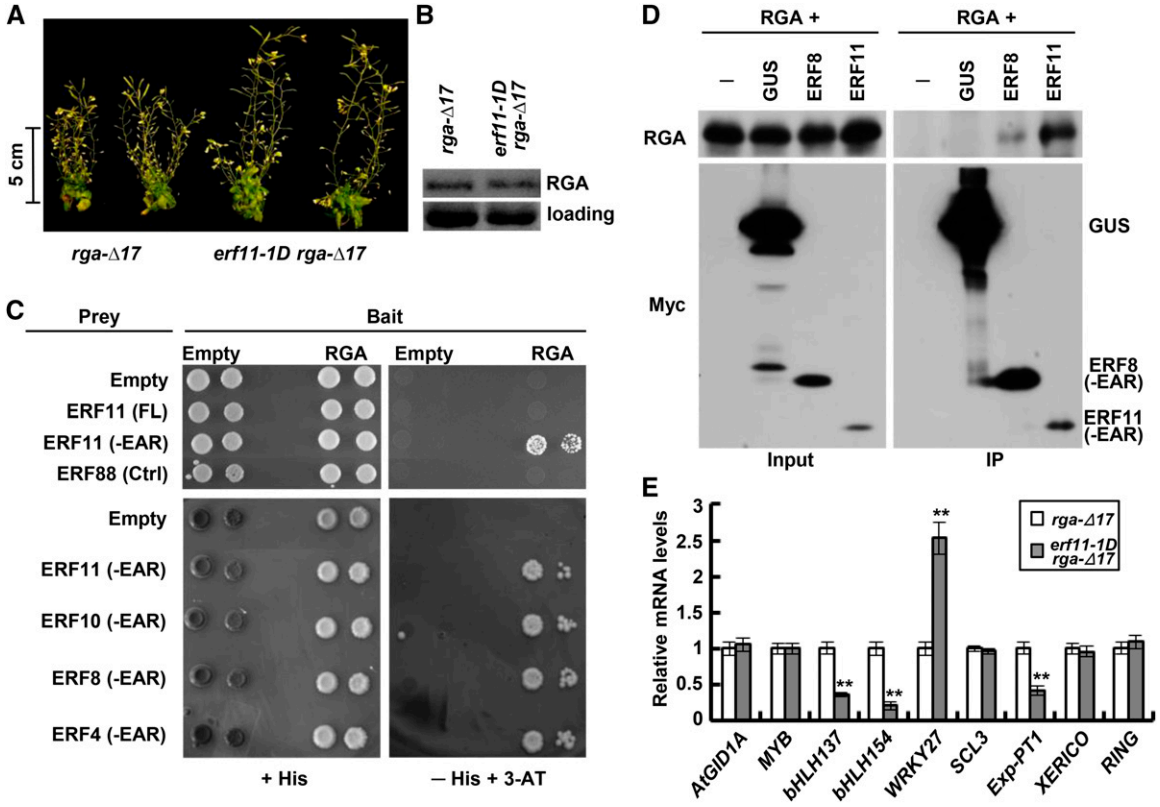

Figure 4. ERF11 interacts with RGA and inhibits its function. A, *erf11-1D* partially rescued the dwarf phenotype of *rga-Δ17*. Image shows 60-d-old plants. B, Similar rga-Δ17 protein levels were present in the upper growing internodes of 70-d-old *rga-Δ17* and *erf11-1D rga-Δ17*. The immunoblot was probed with affinity-purified anti-RGA antibodies. The bottom panel shows equal loading by Ponceau staining. C, Interactions between ERFs and RGA in yeast two-hybrid assays. A truncated RGA protein (amino acids 187 to 587) that contains the C-terminal GRAS domain was used as the bait. ERFs were used as the prey. FL, Full-length; –EAR, EAR motif deleted. For each strain, 2 μL yeast cells with OD_{600} values of 0.25 and 0.025 were spotted on control media (+His) and –His media +1 mM 3-AT (a competitive inhibitor of His-3 enzyme). Empty prey and bait vectors were included as negative controls. D, co-IP of ERFs and RGA in planta. HA-RGA was transiently expressed alone or coexpressed with cMyc-tagged GUS, ERF11 (–EAR), or ERF8 (–EAR) in *N. benthamiana*. The total protein extracts were immunoprecipitated with anti-cMyc antibody-conjugated agarose beads; the input and IP samples were analyzed by immunoblotting using antibodies for HA and cMyc, separately. E, *erf11-1D* reduced the transcript levels of DELLA target genes *bHLH137*, *bHLH154*, and Exp-PT1 in the internodes of 70-d-old *rga-Δ17* plants. RT-qPCR data represent means ± SE of four repeats. $^{**}P < 0.01$. In A, B, and E, *rga-Δ17* is hemizygous in both *rga-Δ17* and *erf11-1D rga-Δ17*.

(Zentella et al., 2007) in *rga-Δ17* and *erf11-1D rga-Δ17* by RT-qPCR analysis (Fig. 4E). We found that expression of three of the DELLA target genes (*bHLH137*, *bHLH154*, and *Exp-PT1*) was down-regulated in the internodes of *erf11-1D rga-Δ17*, suggesting that ERF11 and DELLA interfere with each other's function by direct protein-protein interaction.

To examine further the direct antagonistic interaction between ERF11 and DELLA, these proteins were expressed alone or coexpressed in tobacco leaves by agroinfiltration to test whether they antagonistically modulate transcription of *bHLLH137* and *bHLH154* promoters using the dual luciferase (LUC) reporter assay (Fig. 5). The reporter constructs contain promoter sequences of *bHLH137*, *bHLH154*, and *SCL3* genes, respectively, which were fused to the firefly *LUC* gene (*fLUC*; Fig. 5A). The *SCL3* promoter was included as a control; *SCL3* is an RGA-induced target gene (Zentella et al., 2007), but its expression was not altered by *erf11-1D* (Fig. 4E). The *35S:Renilla LUC* (*rLUC*) was used as an internal standard in the assay. Two effectors are *35S:HA-RGA* and *35S:myc-ERF11*. As expected, expression of RGA alone induced all three promoters of RGA target genes (4-fold for *bHLH137*, 3-fold for *bHLH154*, and 8-fold for *SCL3*) compared to the empty effector control (Fig. 5B). ERF11 alone repressed expression of *bHLH137* by 5-fold, and coexpression of RGA and ERF11 displayed antagonistic effects on the expression of this promoter (Fig. 5B). In contrast, ERF11 did not significantly repress expression of *SCL3*, indicating that the inhibitory effect of ERF11 on the *bHLH137* promoter is specific. We also found that *bHLH154* expression was not affected by ERF11 in the dual luciferase assay (Fig. 5B), suggesting that this gene may not be a direct target of ERF11. The optimal cis-element for ERFs has been identified to be the GCC box (AGCCGCC), although

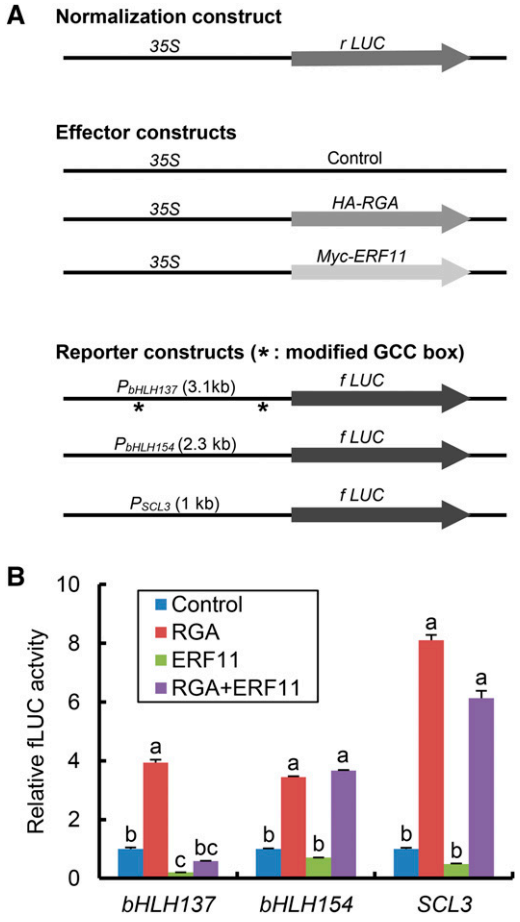

Figure 5. ERF11 repressed, whereas RGA induced, transcription of the *bHLH137* promoter in tobacco transient expression assay by agroinfiltration. A, Schematics of the normalization control, reporter, and effector constructs. *35S:Renilla LUC* (*rLUC*) served to normalize transformation efficiency. In the reporter constructs, the *firefly LUC* gene (*fLUC*) was placed under the control of different promoters of RGA target genes (*bHLH137*, *bHLH154*, and *SCL3*). *35S:RGA* and *35S:ERF11* served as two effector constructs, respectively. The positions of two modified GCC box sequences in *bHLH137* promoter are labeled by asterisks: AGCCGCT at –2 kb and ACCCGCC at –0.2 kb. The empty effector vector was used as a negative control. B, RGA induced expression of all three target gene promoters, whereas ERF11 only repressed *bHLH137* expression. Each reporter construct and the *35S:rLUC* construct were introduced into tobacco leaves in the presence of the empty effector constructs (Control) or *35S:RGA* and/or *35S:ERF11* (with the same molar ratios) by agroinfiltration. The relative fLUC activity (normalized by rLUC activity) in the empty effector control was set to 1. Data represent the average value ± SE of eight biological replicas. Different letters above the bars indicate significant difference ($P < 0.01$).

AtERF3 and AtERF4 can also bind similar sequences with single nucleotide substitutions (Ohme-Takagi and Shinshi, 1995; Fujimoto et al., 2000). Interestingly, using pDRAW32 DNA analysis software (http://www.acaclone.com), we found that the *bHLH137* promoter contains two modified GCC elements (Fig. 5A), whereas the promoters of *bHLH154* and *SCL3* genes lack any putative ERF binding sequences. Taken together, our results show that ERF11 directly represses RGA-induced *bHLH137* expression.

DISCUSSION

The data in this report revealed that ERF11 enhances GA responses by two mechanisms: (1) increasing bioactive GA levels by inducing expression of the GA biosynthesis genes *GA3ox* and *GA20ox* and (2) promoting GA responses by antagonizing the activity of the GA signaling repressor DELLA via direct protein-protein interaction (Fig. 6). Our transient expression assay showed that ERF11 represses whereas DELLA induces transcription of the target gene *bHLH137* (Fig. 5), indicating that ERF11 and DELLA interfere with each other's function. The second mechanism should reduce DELLA function immediately, whereas the first mechanism acts slower in regulating DELLA activity as its effect on DELLA is via alteration in GA biosynthesis. ERF11 is unique in that it promotes both GA biosynthesis and GA signaling. All of the previously reported elevated GA-signaling mutants down-regulate GA biosynthesis via the negative feedback mechanism (Sun and Gubler, 2004). Our data further suggest that induction of GA biosynthesis gene expression by ERF11 is likely an indirect effect mediated by decreasing ethylene levels (Fig. 6). *erf11-1D* conferred a reduction in the amounts of ethylene in the inflorescence stems, consistent with a recent report showing ERF11 represses *ACS* transcription (Li et al., 2011). The exact molecular

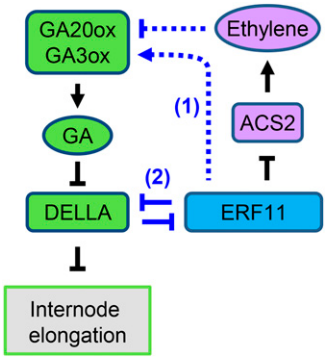

Figure 6. Model for antagonistic interaction between ERF11 and DELLA in regulating GA and ethylene pathways and internode elongation. The arrows and T-bars highlighted in blue represent new links that are revealed in this study. ERF11 promotes internode elongation by enhancing GA responses through two mechanisms: (1) increasing GA accumulation (and therefore DELLA degradation) indirectly via its inhibitory effect on ethylene biosynthesis; and (2) inhibiting DELLA function by direct protein-protein interaction. DELLA and ERF11 antagonize each other's function in regulating downstream gene expression, as shown in the transient expression assay. In (1), ERF11-induced GA accumulation is likely an indirect effect of reduction of ethylene production via inhibition of *ACS2* expression by ERF11. The reduced ethylene levels then result in repression of *GA3ox* and *GA20ox* expression, likely through the ethylene signaling pathway.

mechanism of how ethylene inhibits GA biosynthesis gene expression requires further investigation.

In Arabidopsis, there are 122 ERF/AP2 family members. AtERF11 belongs to the subfamily VIII-B-1a (McGrath et al., 2005; Nakano et al., 2006). All eight members in this subfamily (ERF3, 4, and 7–12) contain a transcription repressor EAR motif near their C terminus. Interestingly, our study and previous reports reveal that three of the EAR-containing ERFs (ERF4, ERF7, and ERF11) regulate multiple hormone pathways. Overexpression of AtERF4 confers reduced sensitivity to ethylene, abscisic acid (ABA), and JA in hypocotyl or root growth, whereas the loss-of-function *erf4-1* mutant displays increased JA response (McGrath et al., 2005; Yang et al., 2005). Overexpression or silencing of *AtERF7* resulted in reduced or increased ABA response in stomatal closure, respectively, indicating that AtERF7 negatively regulates ABA responses (Song et al., 2005). Our data showed that overexpression of ERF11, ERF4, or ERF8 partially rescued the dwarf phenotype of the GA-deficient *ga1-6* mutant. Phenotype analyses of the loss-of-function *erf11* and *erf4* single and double mutants further confirmed that ERF4 and ERF11 positively regulate GA response in hypocotyl elongation. Similar to ERF11, ERF4, 8, and 10 interact with DELLA in co-IP and/or yeast two-hybrid assays. Future studies will determine whether all eight VIII-B-1a subfamily ERFs regulate GA and/or other hormone pathways by a similar mechanism as illustrated for ERF11. Our yeast two-hybrid results indicate that RGA does not interact with ERF88 in the VIII-B-1b subfamily. Interestingly, a group-VII ERF/AP2 (RELATED TO APETALA2.3) was shown recently to be a DELLA-interacting protein, playing a role in GA and ethylene-regulated apical hook development (Marín-de la Rosa et al., 2014). Future studies will address whether any of the other ERF/AP2 subfamily members are DELLA-interacting proteins.

In rice (*Oryza sativa*), group VII ERFs (OsSUB1A, SNORKEL1, and SNORKEL2) that lack the EAR motif have been shown to regulate internode elongation that is modulated by ethylene and GA (Xu et al., 2006; Hattori et al., 2009). Interestingly, these OsERFs (transcription activators) function differently from AtERF11. In submergence-tolerant rice, ethylene inhibits internode growth under submergence conditions. In this case, ethylene induces OsSUB1A expression (Xu et al., 2006), which in turn inhibits GA response by promoting *SLR1* (rice DELLA) and *SLRL1* transcript and protein accumulation (Fukao and Bailey-Serres, 2008). Ectopic expression of OsSUB1A in Arabidopsis leads to reduced GA response and increased ABA response (Fukao et al., 2011). In contrast to the submergence-tolerant rice, deepwater rice responds to submergence by rapid internode growth. In this case, ethylene promotes internode elongation by increasing GA levels via induction of SNORKEL1 and SNORKEL2 expression, although it is unclear how SNORKEL1 and SNORKEL2 promote GA accumulation (Hattori et al., 2009). Therefore, different members of the group VII ERFs play distinct roles in mediating ethylene and GA responses in controlling internode elongation.

In summary, increasing numbers of ERFs have been shown to regulate plant development in response to hormonal signals or abiotic stresses. Our work reveals that AtERF11 promotes internode elongation by promoting both GA biosynthesis and signaling pathways.

MATERIALS AND METHODS

Plant Materials and Growth Conditions

The *ga1-6* semidwarf mutant plant used for activation tagging was generated by crossing the original *ga1-6* in the Landsberg *erecta* (L*er*) background (Koornneef and van der Veen, 1980; Sun and Kamiya, 1994) four times into Columbia-0 (Col-0). The activation-tagging mutant pools were generated by transforming *ga1-6* (4x Col-0) with pSKI015 (Weigel et al., 2000), and the mutant #279-2 was identified in the T1 generation as a BASTA-resistant plant that was taller than the parental plant. #279-2 displayed a 3:1 segregation ratio of the BASTA resistance in the T2 generation; homozygous lines were identified by screening in the T3 generation (renamed *erf11-1D ga1-6*). The *erf11* (SALK_116053) T-DNA insertion mutant was requested from the Arabidopsis Stock Center, and the *erf4-1* (Salk_073394) mutant was provided by Dr. Kemal Kazan (McGrath et al., 2005). The homozygous double mutant *erf4 erf11* was generated by crossing *erf11* to *erf4*. The *erf11-1D rga-Δ17* double mutant was generated by crossing a *rga-Δ17* transgenic line (#18-2-1) in the Col-0 background (Dill et al., 2001) to *erf11-1D*. Genotyping primers are listed in Supplemental Table S2.

For growth on media, seeds were plated on 1× or 0.5× Murashige and Skoog (MS) medium containing 2% or 1% Suc and 0.7% agar, and incubated at 22°C under constant light (50–70 μmol m^{-2} s^{-1}). For growth on soil, seeds were sown on MetroMix 200 (Sun Gro Horticulture) and incubated at 22°C under 16 h light. The procedure for the hypocotyl elongation assay was described previously (Zhang et al., 2011). For ethylene-mediated seedling triple-response assay, the detailed procedure was described before (Zhou et al., 2007). Seeds were stratified at 4°C for 72 h and then germinated on half-strength MS at 22°C for 80 h in the dark with or without 20 μL/L ethylene gas. Dark-grown seedlings were photographed and hypocotyl length was measured using software Image J. Transgenic Arabidopsis lines were generated by the floral dip method (Clough and Bent, 1998). For selection, 10 μg/mL of BASTA or 50 μg/mL kanamycin was included in the MS medium.

All statistical analyses were performed using Student's *t* tests with the statistical package JMP Pro 10.0.2 (SAS Institute).

Plasmid Constructs

All the primers used in this study are listed in Supplemental Table S2. The PCR-amplified fragments in all constructs were sequenced to ensure that no mutations were introduced. Detailed information on plasmid construction is described in Supplemental Methods.

TAIL-PCR

Genomic DNA was extracted by using the CTAB method (Weigel and Glazebrook, 2002). TAIL-PCR was carried out as described previously (Liu et al., 1995). The degenerate primers used for TAIL-PCR were AD1, AD2, and AD3 (Liu and Whittier, 1995) and AD4 and AD6 (Liu et al., 1995). The T-DNA specific primers LB8, LB7, and JL-202 (Alonso et al., 2003) were used in the primary, secondary, and tertiary TAIL-PCR reactions, respectively. Specific TAIL-PCR products were gel-purified and sequenced and BLAST searched against the National Center for Biotechnology Information database to identify the T-DNA insertion site.

Quantitative Real-Time RT-PCR Analysis

The real-time RT-qPCR analyses were performed with an Eppendorf realplex2 Mastercycler ep gradient S. Total RNA isolation, cDNA synthesis, and qPCR analyses were performed as described previously (Zentella et al., 2007). At4g33380, whose expression remains constant (Rieu et al., 2008b), was used as

the control to normalize the qPCR data. Unless specified otherwise, the qPCR data are the means of four repeats (two biological repeats and two technical replicates of each set of samples).

GA Measurements

Rosette leaves of 33-d-old soil-grown *ga1-6* and *erf11-1D ga1-6* plants were harvested and immediately frozen in liquid nitrogen and lyophilized. GAs were purified and quantified according to Plackett et al. (2012) using a 6410 Triple Quad LC-MS (Agilent Technologies) with an Agilent 1200 series rapid resolution liquid chromatography system fitted with a Zorbax SB-Phenyl column (1.8 μm, 2.1 $\times$ 50 mm).

Immunoblot Analyses

Total proteins from seedlings or internodes were extracted as described before (Silverstone et al., 2001). The extracted proteins were fractionated by 8% SDS-PAGE and analyzed by immunoblot analysis using anti-HA antibodies (Covance) or crude anti-RGA antibodies (Silverstone et al., 2001).

Yeast Two-Hybrid Assays

The yeast two-hybrid assay was performed using the ProQuest system (Invitrogen) in the yeast strain pJ69-4A (James et al., 1996). Varying concentrations of 3-AT (0, 1, 2.5, 5, 10, and 25 mM) were included in medium lacking Trp, Leu, and His. For each combination, 2 μL yeast cells with OD_{600} values of 0.25 and 0.025, respectively, were spotted on media plates.

Coimmunoprecipitation of ERFs and RGA, and Dual Luciferase Assay

Transient expression and co-IP assays were performed as described previously (Zhang et al., 2011) with the following modifications: After cells were resuspended in infiltration media, *Agrobacterium tumefaciens* GV3101 strains carrying individual expression constructs were mixed to make a final OD_{600} of about 0.8 for each strain and infiltrated into 28-d-old *Nicotiana benthamiana* (tobacco) leaves by needle-less syringe; 40 h transiently transformed tobacco leaves were harvested for co-IP assay without cross-linking. Two grams of leaves was ground into a fine powder in liquid nitrogen, followed by resuspension in 5 mL extraction buffer (50 mM Tris, pH 7.5, 150 mM NaCl, 1% Triton X-100, 5 mM β-mercaptoethanol, and 1$\times$ Protease Inhibitors [Sigma P-9599]). The powder was ground in extraction buffer for 10 min on ice until there was no visible debris. The homogenates were centrifuged at 20,000*g* at 4°C for 20 min. The co-IP was performed using 10 μL anti-cMyc agarose-conjugated beads (A7470; Sigma-Aldrich) by incubating with supernatant for 2 h at 4°C.

The dual luciferase assays were also performed using the transient expression system in tobacco. The control constructs and the reporter and effector constructs were individually transformed into *Agrobacterium* strain GV3101. Then, each reporter- and *rLUC*-containing strain was coinfiltrated into tobacco leaves with various combinations of effector strains. Forty hours after infiltration, tobacco leaves were harvested for protein extraction, and luciferase activities were measured using the dual-luciferase reporter assay system (Promega). Relative promoter activity was calculated as the ratio of fLUC to rLUC activities for each sample. Six biological repeats were conducted for each effector combination.

Ethylene Measurement

The top 10 internodes of the main stems were detached, and the flower clusters and siliques were removed. For each set of measurements, 15 stems (per genotype) were placed in a 22-mL gas chromatography vial containing 0.5 mL of 0.5$\times$ liquid MS media. The vials were capped and then placed in a 16-h/8-h light/dark cycle incubator at 22°C for 5 h. The accumulated ethylene was measured and calculated based on comparison to a 1 mL/L ethylene standard (Woeste et al., 1999). Data were from three replicates, and each experiment was repeated at least once with comparable results.

Cell Length Measurement by Scanning Electron Microscopy

The 10th to 20th internodes from the bottom on the main stem of 70-d-old *ga1-6* and *erf11-1D ga1-6* plants were fixed overnight with FAA solution (5% acetic acid, 45% ethanol, and 5% formaldehyde) and dehydrated with a graded ethanol series (30%, 50%, 70%, 90%, and 100%) (Tsukaya et al., 1993). After dehydration, the samples were chemically dried with HMDS (hexamethyldisilazane) and then were imaged on an FEI XL30 ESEM.

Accession Numbers

Arabidopsis Genome Initiative locus identifiers for the genes mentioned in this article are as follows: *ERF11* (At1g28370), *ERF4* (At3g15210), *ERF8* (At1g53170), *ERF10* (At1g03800), *ERF12* (At1g28360), *ERF88* (At1g12890), *ACS2* (At1g01480), *GA1* (At4g02780), *RGA* (At2g01570), *GAI* (At1g14920), *GA3ox1* (At1g15550), *GA3ox2* (At1g80340), *GA20ox1* (At4g25420), *GA20ox2* (At5g51810), *GA2ox6* (At1g02400), *AtGID1A* (At3g05120), *MYB* (At3g11280), *bHLH137* (At5g50915), *bHLH154* (At2g31730), *WRKY27* (At5g52830), *SCL3* (At1g50420), *EXP-PT1* (At2g45900), *XERICO* (At2g04240), *RING* (At4g19700), *EXP-PT* (At4g33380), and unknown protein (At1g28375).

Supplemental Data

The following supplemental materials are available.

Supplemental Figure S1. Characterization of *ERF* Overexpression Lines and *erf* Loss-of-Function Mutants.

Supplemental Figure S2. *erf11-1D* Caused an Elevated GA Response and Reduced Levels of RGA Protein.

Supplemental Figure S3. *erf11-1D* Partially Rescued *rga-Δ17* Phenotypes.

Supplemental Figure S4. Interactions between ERFs and GAI in Yeast Two-Hybrid Assays.

Supplemental Table S1. Silique and Flowering Time Phenotypes of *ga1-6* and *erf11-1D ga1-6*.

Supplemental Table S2. List of Primers and Their Uses.

Supplemental Methods, Figure Legends, and References.

ACKNOWLEDGMENTS

We are grateful to Joe Kieber and Gyeong Mee Yoon for their advice with ethylene analyses and for providing the facility for ethylene measurements. We thank Benke Kuai for his generous support of some of the ethylene-related studies, and Tomoe Nose and Yumiko Takebayashi for technical support in LC-MS/MS hormone analysis. We also thank Kemal Kazan for *erf4-1*, Jian-Min Zhou for *ein3* and *EIN3-OE* lines, Chi-Kuang Wen for helpful discussions, and Michelle Gignac at the SEM facility at Duke for help with scanning electron microscopy analysis.

Received February 4, 2016; accepted May 30, 2016; published June 2, 2016.

LITERATURE CITED

Achard P, Baghour M, Chapple A, Hedden P, Van Der Straeten D, Genschik P, Moritz T, Harberd NP (2007) The plant stress hormone ethylene controls floral transition via DELLA-dependent regulation of floral meristem-identity genes. Proc Natl Acad Sci USA **104:** 6484–6489

Alonso JM, Stepanova AN, Leisse TJ, Kim CJ, Chen H, Shinn P, Stevenson DK, Zimmerman J, Barajas P, Cheuk R, et al (2003) Genome-wide insertional mutagenesis of *Arabidopsis thaliana.* Science **301:** 653–657

An F, Zhang X, Zhu Z, Ji Y, He W, Jiang Z, Li M, Guo H (2012) Coordinated regulation of apical hook development by gibberellins and ethylene in etiolated Arabidopsis seedlings. Cell Res **22:** 915–927

Bai MY, Shang JX, Oh E, Fan M, Bai Y, Zentella R, Sun T, Wang Z-Y (2012) Brassinosteroid, gibberellin, and phytochrome impinge on a common transcription module in Arabidopsis. Nat Cell Biol **14:** 810–817

Clough SJ, Bent AF (1998) Floral dip: a simplified method for *Agrobacterium*-mediated transformation of *Arabidopsis thaliana.* Plant J **16:** 735–743

Davière JM, Achard P (2016) A pivotal role of DELLAs in regulating multiple hormone signals. Mol Plant **9:** 10–20

de Lucas M, Davière JM, Rodríguez-Falcón M, Pontin M, Iglesias-Pedraz JM, Lorrain S, Fankhauser C, Blázquez MA, Titarenko E, Prat S (2008) A molecular framework for light and gibberellin control of cell elongation. Nature **451:** 480–484

Dill A, Jung H-S, Sun TP (2001) The DELLA motif is essential for gibberellin-induced degradation of RGA. Proc Natl Acad Sci USA **98:** 14162–14167

Dill A, Sun T (2001) Synergistic derepression of gibberellin signaling by removing RGA and GAI function in *Arabidopsis thaliana*. Genetics **159:** 777–785

Feng S, Martinez C, Gusmaroli G, Wang Y, Zhou J, Wang F, Chen L, Yu L, Iglesias-Pedraz JM, Kircher S, et al (2008) Coordinated regulation of *Arabidopsis thaliana* development by light and gibberellins. Nature **451:** 475–479

Fujimoto SY, Ohta M, Usui A, Shinshi H, Ohme-Takagi M (2000) Arabidopsis ethylene-responsive element binding factors act as transcriptional activators or repressors of GCC box-mediated gene expression. Plant Cell **12:** 393–404

Fukao T, Bailey-Serres J (2008) Submergence tolerance conferred by Sub1A is mediated by SLR1 and SLRL1 restriction of gibberellin responses in rice. Proc Natl Acad Sci USA **105:** 16814–16819

Fukao T, Yeung E, Bailey-Serres J (2011) The submergence tolerance regulator SUB1A mediates crosstalk between submergence and drought tolerance in rice. Plant Cell **23:** 412–427

Griffiths J, Murase K, Rieu I, Zentella R, Zhang ZL, Powers SJ, Gong F, Phillips AL, Hedden P, Sun TP, Thomas SG (2006) Genetic characterization and functional analysis of the GID1 gibberellin receptors in Arabidopsis. Plant Cell **18:** 3399–3414

Hattori Y, Nagai K, Furukawa S, Song XJ, Kawano R, Sakakibara H, Wu J, Matsumoto T, Yoshimura A, Kitano H, et al (2009) The ethylene response factors SNORKEL1 and SNORKEL2 allow rice to adapt to deep water. Nature **460:** 1026–1030

Hou X, Lee LY, Xia K, Yan Y, Yu H (2010) DELLAs modulate jasmonate signaling via competitive binding to JAZs. Dev Cell **19:** 884–894

Itoh H, Ueguchi-Tanaka M, Sato Y, Ashikari M, Matsuoka M (2002) The gibberellin signaling pathway is regulated by the appearance and disappearance of SLENDER RICE1 in nuclei. Plant Cell **14:** 57–70

James P, Halladay J, Craig EA (1996) Genomic libraries and a host strain designed for highly efficient two-hybrid selection in yeast. Genetics **144:** 1425–1436

King KE, Moritz T, Harberd NP (2001) Gibberellins are not required for normal stem growth in *Arabidopsis thaliana* in the absence of GAI and RGA. Genetics **159:** 767–776

Koornneef M, van der Veen JH (1980) Induction and analysis of gibberellin sensitive mutants in *Arabidopsis thaliana* (L.) heynh. Theor Appl Genet **58:** 257–263

Li Z, Zhang L, Yu Y, Quan R, Zhang Z, Zhang H, Huang R (2011) The ethylene response factor AtERF11 that is transcriptionally modulated by the bZIP transcription factor HY5 is a crucial repressor for ethylene biosynthesis in Arabidopsis. Plant J **68:** 88–99

Lim S, Park J, Lee N, Jeong J, Toh S, Watanabe A, Kim J, Kang H, Kim DH, Kawakami N, Choi G (2013) ABA-insensitive3, ABA-insensitive5, and DELLAs Interact to activate the expression of SOMNUS and other high-temperature-inducible genes in imbibed seeds in Arabidopsis. Plant Cell **25:** 4863–4878

Liu Y-G, Mitsukawa N, Oosumi T, Whittier RF (1995) Efficient isolation and mapping of *Arabidopsis thaliana* T-DNA insert junctions by thermal asymmetric interlaced PCR. Plant J **8:** 457–463

Liu Y-G, Whittier RF (1995) Thermal asymmetric interlaced PCR: automatable amplification and sequencing of insert end fragments from P1 and YAC clones for chromosome walking. Genomics **25:** 674–681

Locascio A, Blázquez MA, Alabadí D (2013) Dynamic regulation of cortical microtubule organization through prefoldin-DELLA interaction. Curr Biol **23:** 804–809

Marín-de la Rosa N, Pfeiffer A, Hill K, Locascio A, Bhalerao RP, Miskolczi P, Grønlund AL, Wanchoo-Kohli A, Thomas SG, Bennett MJ, et al (2015) Genome wide binding site analysis reveals transcriptional coactivation of cytokinin-responsive genes by DELLA proteins. PLoS Genet **11:** e1005337

Marín-de la Rosa N, Sotillo B, Miskolczi P, Gibbs DJ, Vicente J, Carbonero P, Oñate-Sánchez L, Holdsworth MJ, Bhalerao R, Alabadí D, Blázquez MA (2014) Large-scale identification of gibberellin-related transcription factors defines group VII ETHYLENE RESPONSE FACTORS as functional DELLA partners. Plant Physiol **166:** 1022–1032

McGrath KC, Dombrecht B, Manners JM, Schenk PM, Edgar CI, Maclean DJ, Scheible WR, Udvardi MK, Kazan K (2005) Repressor- and activator-type ethylene response factors functioning in jasmonate signaling and disease resistance identified via a genome-wide screen of Arabidopsis transcription factor gene expression. Plant Physiol **139:** 949–959

Mitchum MG, Yamaguchi S, Hanada A, Kuwahara A, Yoshioka Y, Kato T, Tabata S, Kamiya Y, Sun TP (2006) Distinct and overlapping roles of two gibberellin 3-oxidases in Arabidopsis development. Plant J **45:** 804–818

Murase K, Hirano Y, Sun TP, Hakoshima T (2008) Gibberellin-induced DELLA recognition by the gibberellin receptor GID1. Nature **456:** 459–463

Nakano T, Suzuki K, Fujimura T, Shinshi H (2006) Genome-wide analysis of the ERF gene family in Arabidopsis and rice. Plant Physiol **140:** 411–432

Ohme-Takagi M, Shinshi H (1995) Ethylene-inducible DNA binding proteins that interact with an ethylene-responsive element. Plant Cell **7:** 173–182

Park J, Nguyen KT, Park E, Jeon JS, Choi G (2013) DELLA proteins and their interacting RING Finger proteins repress gibberellin responses by binding to the promoters of a subset of gibberellin-responsive genes in Arabidopsis. Plant Cell **25:** 927–943

Plackett ARG, Powers SJ, Fernandez-Garcia N, Urbanova T, Takebayashi Y, Seo M, Jikumaru Y, Benlloch R, Nilsson O, Ruiz-Rivero O, et al (2012) Analysis of the developmental roles of the Arabidopsis gibberellin 20-oxidases demonstrates that GA20ox1, -2, and -3 are the dominant paralogs. Plant Cell **24:** 941–960

Rieu I, Eriksson S, Powers SJ, Gong F, Griffiths J, Woolley L, Benlloch R, Nilsson O, Thomas SG, Hedden P, Phillips AL (2008a) Genetic analysis reveals that C19-GA 2-oxidation is a major gibberellin inactivation pathway in Arabidopsis. Plant Cell **20:** 2420–2436

Rieu I, Ruiz-Rivero O, Fernandez-Garcia N, Griffiths J, Powers SJ, Gong F, Linhartova T, Eriksson S, Nilsson O, Thomas SG, Phillips AL, Hedden P (2008b) The gibberellin biosynthetic genes *AtGA20ox1* and *AtGA20ox2* act, partially redundantly, to promote growth and development throughout the Arabidopsis life cycle. Plant J **53:** 488–504

Sarnowska EA, Rolicka AT, Bucior E, Cwiek P, Tohge T, Fernie AR, Jikumaru Y, Kamiya Y, Franzen R, Schmelzer E, et al (2013) DELLA-interacting SWI3C core subunit of switch/sucrose nonfermenting chromatin remodeling complex modulates gibberellin responses and hormonal cross talk in Arabidopsis. Plant Physiol **163:** 305–317

Shimada A, Ueguchi-Tanaka M, Nakatsu T, Nakajima M, Naoe Y, Ohmiya H, Kato H, Matsuoka M (2008) Structural basis for gibberellin recognition by its receptor GID1. Nature **456:** 520–523

Silverstone AL, Jung H-S, Dill A, Kawaide H, Kamiya Y, Sun TP (2001) Repressing a repressor: gibberellin-induced rapid reduction of the RGA protein in Arabidopsis. Plant Cell **13:** 1555–1566

Song CP, Agarwal M, Ohta M, Guo Y, Halfter U, Wang P, Zhu JK (2005) Role of an Arabidopsis AP2/EREBP-type transcriptional repressor in abscisic acid and drought stress responses. Plant Cell **17:** 2384–2396

Sun T, Goodman HM, Ausubel FM (1992) Cloning the Arabidopsis *GA1* locus by genomic subtraction. Plant Cell **4:** 119–128

Sun TP, Gubler F (2004) Molecular mechanism of gibberellin signaling in plants. Annu Rev Plant Biol **55:** 197–223

Sun TP, Kamiya Y (1994) The Arabidopsis *GA1* locus encodes the cyclase *ent*-kaurene synthetase A of gibberellin biosynthesis. Plant Cell **6:** 1509–1518

Tian C, Wan P, Sun S, Li J, Chen M (2004) Genome-wide analysis of the GRAS gene family in rice and Arabidopsis. Plant Mol Biol **54:** 519–532

Tsukaya H, Naito S, Redei GP, Komeda Y (1993) A new class of mutations in *Arabidopsis thaliana, acaulis1*, affecting the development of both inflorescences and leaves. Development **118:** 751–764

Ueguchi-Tanaka M, Ashikari M, Nakajima M, Itoh H, Katoh E, Kobayashi M, Chow TY, Hsing YI, Kitano H, Yamaguchi I, Matsuoka M (2005) *GIBBERELLIN INSENSITIVE DWARF1* encodes a soluble receptor for gibberellin. Nature **437:** 693–698

Ueguchi-Tanaka M, Nakajima M, Motoyuki A, Matsuoka M (2007) Gibberellin receptor and its role in gibberellin signaling in plants. Annu Rev Plant Biol **58:** 183–198

Weigel D, Ahn JH, Blázquez MA, Borevitz JO, Christensen SK, Fankhauser C, Ferrándiz C, Kardailsky I, Malancharuvil EJ, Neff MM, et al (2000) Activation tagging in Arabidopsis. Plant Physiol **122:** 1003–1013

Weigel D, Glazebrook J (2002) Arabidopsis: A Laboratory Manual. Cold Spring Harbor Laboratory Press, Cold Spring Harbor, NY

Woeste KE, Vogel JP, Kieber JJ (1999) Factors regulating ethylene biosynthesis in etiolated Arabidopsis thaliana seedlings. Physiol Plant **105:** 478–484

Xu H, Liu Q, Yao T, Fu X (2014) Shedding light on integrative GA signaling. Curr Opin Plant Biol **21:** 89–95

Xu K, Xu X, Fukao T, Canlas P, Maghirang-Rodriguez R, Heuer S, Ismail AM, Bailey-Serres J, Ronald PC, Mackill DJ (2006) Sub1A is an ethylene-response-factor-like gene that confers submergence tolerance to rice. Nature **442:** 705–708

Yang DL, Yao J, Mei CS, Tong XH, Zeng LJ, Li Q, Xiao LT, Sun TP, Li J, Deng XW, et al (2012) Plant hormone jasmonate prioritizes defense over growth by interfering with gibberellin signaling cascade. Proc Natl Acad Sci USA **109:** E1192–E1200

Yang Z, Tian L, Latoszek-Green M, Brown D, Wu K (2005) Arabidopsis ERF4 is a transcriptional repressor capable of modulating ethylene and abscisic acid responses. Plant Mol Biol **58:** 585–596

Zentella R, Zhang ZL, Park M, Thomas SG, Endo A, Murase K, Fleet CM, Jikumaru Y, Nambara E, Kamiya Y, Sun TP (2007) Global analysis of DELLA direct targets in early gibberellin signaling in Arabidopsis. Plant Cell **19:** 3037–3057

Zhang D, Jing Y, Jiang Z, Lin R (2014) The chromatin-remodeling factor PICKLE integrates brassinosteroid and gibberellin signaling during skotomorphogenic growth in Arabidopsis. Plant Cell **26:** 2472–2485

Zhang ZL, Ogawa M, Fleet CM, Zentella R, Hu J, Heo J-O, Lim J, Kamiya Y, Yamaguchi S, Sun T (2011) SCARECROW-LIKE 3 promotes gibberellin signaling by antagonizing DELLA in Arabidopsis. Proc Natl Acad Sci USA **108:** 2160–2165

Zhou X, Liu Q, Xie F, Wen CK (2007) RTE1 is a Golgi-associated and ETR1-dependent negative regulator of ethylene responses. Plant Physiol **145:** 75–86